LA-UR-95- 554

Conf-9503107--1

TITLE: THE LOS ALAMOS PHOTON COUNTING DETECTOR DEBRIS DETECTION PROJECT: AN UPDATE

AUTHOR(S): Cheng Ho
William Priedhorsky
Miles Baron
Don Casperson

SUBMITTED TO: 13th Space Survelliance Workshop
Lexington, MA
March 28-30, 1995

MASTER

Los Alamos
NATIONAL LABORATORY

DISTRIBUTION OF THIS DOCUMENT IS UNLIMITED

Form No. 836 R5
ST 2629 10/91

DISCLAIMER

The Los Alamos Photon Counting Detector Debris Detection Project: An Update

Cheng Ho, Bill Priedhorsky, Miles Baron, Don Casperson

(Los Alamos National Laboratory, MS D436, Los Alamos, NM 87545)

ABSTRACT

At Los Alamos, we have been pursuing a project for space debris detection using a photon counting detector with high spatial and time resolution. By exploiting the three dimensionality of the high quality data, we expect to be able to detect an orbiting object of size below 2 cm, using a moderate size telescope and state-of-the-art photon counting detector. A working tube has been used to collect skyward looking data during dusk. In this paper, we discuss the progress in the development of detector and data acquisition system. We also report on analysis and results of these data sets.

1. DETECTION CONCEPT

During dawn and dusk, a telescope located on the night side of the earth can detect sunlight reflected by an object in low-earth orbit. The orbiting object moving at a high velocity relative to a fixed background of stars and diffuse light provides a unique signature for detection. It is, however, difficult to detect small objects with an imaging detector collecting 2-dimensional data: the faint track left by a small debris with length corresponding to the image integration time will be overwhelmed by the background. With the advance of fast imaging photon counting detector, the data can be collected, instead, in a 3-dimensional format, i.e. (x, y, t) of individual photons. This additional dimensionality greatly enhances the statistical significance of linear features in the data. The purpose of this project is to demonstrate this detection concept. For more details of the scheme, see Ref. 1.

2. PROJECT OVERVIEW AND EXPERIMENTAL SETUP

Since 1993, Los Alamos National Laboratory, with support from the US Air Force Phillips Laboratory, has been pursuing an end-to-end brassboard demonstration of this detection concept, utilizing the microchannel plate/crossed delay line (MCP/CDL) detector under development for DOE programs (Ref. 2). Expected performance of the detector is: active area of 40 mm diameter, about 20 microns FWHM spatial resolution, average quantum efficiency of about 10% depending on the photocathode, much better than 1 millisecond time resolution, and a maximum count rate of 5×10^5 cts/sec. We are currently developing the next generation of electronics which will allow us to push the maximum count rate to well above 10^6 cts/sec. A baseline debris detection system will incorporate a moderate size telescope with the detector, coupled to a fast data acquisition system with large storage capacity.

At the moment, we have one working sealed tube. An end-to-end system from telescope to detector the data acquisition and analysis system has been constructed. The system has been taken to a dark site near Los Alamos on moonless nights for observation in three separate field trips. During each field trip, we pointed the telescope skyward to acquire data

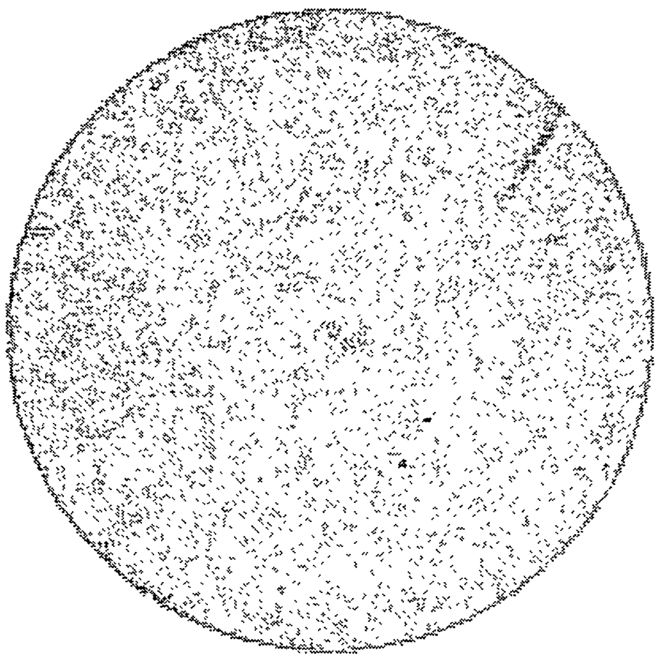

Fig. 1 – Raw *negative* image of the data set collected at 21:45 on July 5, 1994.

suitable for debris detection. In the rest of this paper, we describe the detailed experiment set up and results for one particular exposure. During most of the field trips, the MCP/CDL detector was mounted on a primary telescope which is attached to a portable mount. The telescope consists of a 15 cm aperture Melles Griot lens with 1 m focal length. The site is located at longitude 106.23° West and latitude 35.77° North.

On July 5, 1994, at around 21:45 local Mountain Daylight Saving Time, the telescope was pointed at an elevation of about 57.8° and azimuth of 107.1°. This pointing was selected since the ALEXIS satellite (Ref. 3) was scheduled to pass over at this maximum point with favorable viewing angle. The telescope mount is steerable. During this observation, it was set at a fixed pointing relative to the earth. The data were acquired in a mode which continues until 128 MBytes of RAM (random access memory) in the data acquisition system is filled. Taking into account data recording headers, the entire data set contains about 8 million recorded events, with each raw photon events requiring 8 bytes. The entire exposure lasted 413 seconds. The digital data acquisition electronics provides time resolution of 100 microsecond. As a result of instrument adjustment immediately prior to the exposure, the detector was left at a position focussed at a distance of several hundred meters instead of infinity. As we will see, this blurred the stellar images and reduced the detection sensitivity. A green filter with transmission (> 50%) between 480 and 616 nm was placed in the light path.

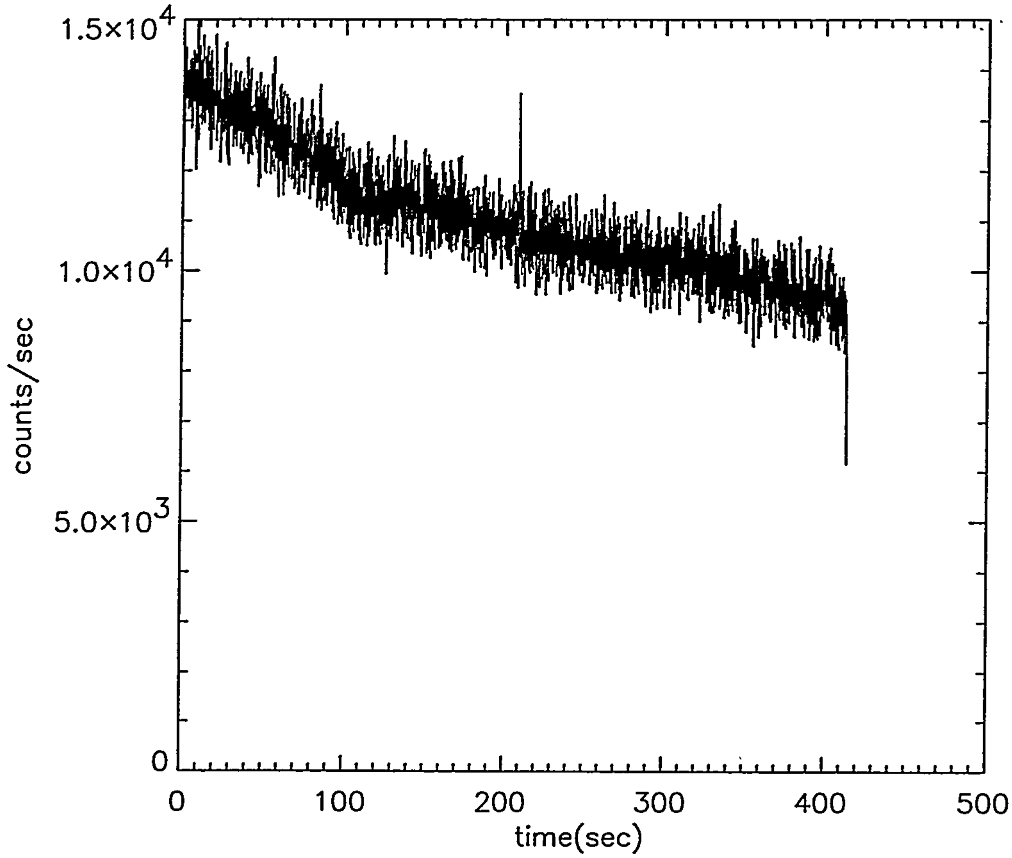

Fig. 2 – Time history of the data set collected at 21:45 on July 5, 1994.

3. ANALYSIS AND RESULTS

The raw *negative* image of this data set following standard reduction and analysis procedures is shown in Figure 1. (In this paper, images are shown as negatives, i.e. visually darker pixels have higher intensity.) In this image, several defects in the detector are easily visible. 1) The diagonal band from upper left to lower right results from gain suppression in MCP due to over-exposing of the tube to UV light. 2) The dark spots throughout the entire image are believed to be dead spots on the photocathode. 3) The two bright spots in the lower right quadrant are believed to be hot spots in the MCP. Furthermore, the window of the detector induces scattered light near the edge of the detector's active area. To eliminate these contaminating artifacts, photon events near the edge were removed in software, reducing the active area to about 35 mm diameter, with a corresponding field of view of about 2 degrees. The total count in the reduced data set is about 4.5×10^6 counts.

The streaks going from the lower left to the upper right are stars in the FOV. The direction of the apparent motion of the stars, due to the earth's rotation, is from the lower

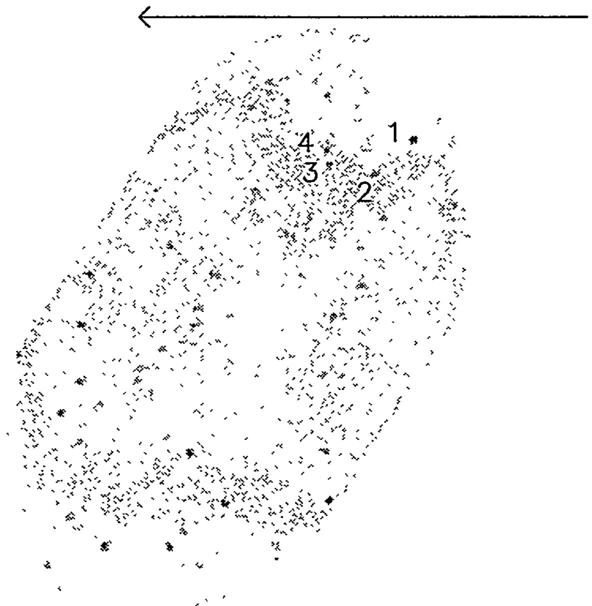

Fig. 3 – Sky image after correction for the earth's motion. See Table 1 for a partial list of identified stars.

Table 1. Identified Stars in FOV

Star Number	Designation	R.A.	Dec.	V Magnitude
1	HR6638	$17^h48.4^m$	20°34′	5.69
2	SAO85445	$17^h49.6^m$	20°38′	7.6
3	SAO85452	17^h50^m	20°52′	7.9
4	SAO85448	$17^h49.7^m$	20°55′	8.0

left (east) to the upper right (west). The time history of the entire reduced data set is shown in Figure 2, with the sky darkening easily visible.

Given the fine time resolution, we can apply a correction for the earth's motion. After re-registering each photon's position as a function of time, we get the image shown in Figure 3. It is straightforward to identify individual stars. Table 1 gives a partial listing of identified stars. Analysis of the image shows that the 5.7 mag star HR6638 yields a count

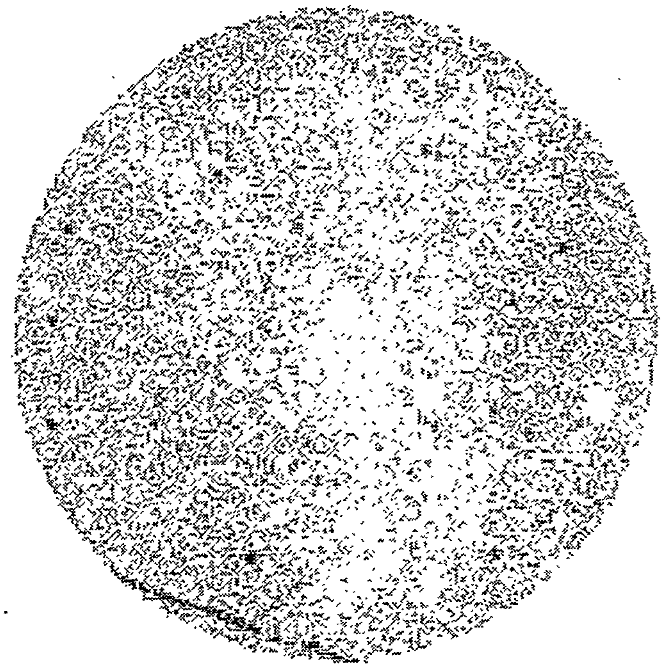

Fig. 4 – Raw image between 206 and 210 seconds of the data set.

rate of about 300 counts/sec. The full width half maximum (FWHM) of the reconstructed stellar image is about 370 microns or 1.25 arcmin. This is consistent with the detector located at an image plane whose conjugate is at about 400 m. (Skyward looking data sets taken later in the same night indicate a point source FWHM of abut 70 microns, consistent with laboratory measurement made under the operating configuration.) From Figure 2, the average count rate during the exposure is about 10^4 counts/sec. Ignoring the difference in color and scaling to HR6638, we estimate the sky brightness to be about 21 mag/square arcsec.

After reviewing the emphemerus of the ALEXIS satellite, it was realized that the exposure started about 30 seconds after the satellite has passed the maximum elevation. The ALEXIS satellite's trajectory would cross the sky shown as the horizontal arrow in Figure 3.

An examination of the time history of the observing run (Fig. 2) reveals a very significant increase in count rate at around 209 seconds after the start of the exposure. Figure 4 shows the raw 2D image of the data set between 206 and 210 second. A linear track is clearly visible. Figure 5 shows the 3 dimensional view of the same data set. The 3D view confirms that the 2D linear feature in Figure 4 is indeed a linear track in the 3D space, indicating that this is a fast moving foreground object in a low-earth orbit. It is easy to envision rotating this data set until the projected plane is normal to this linear track. Figure

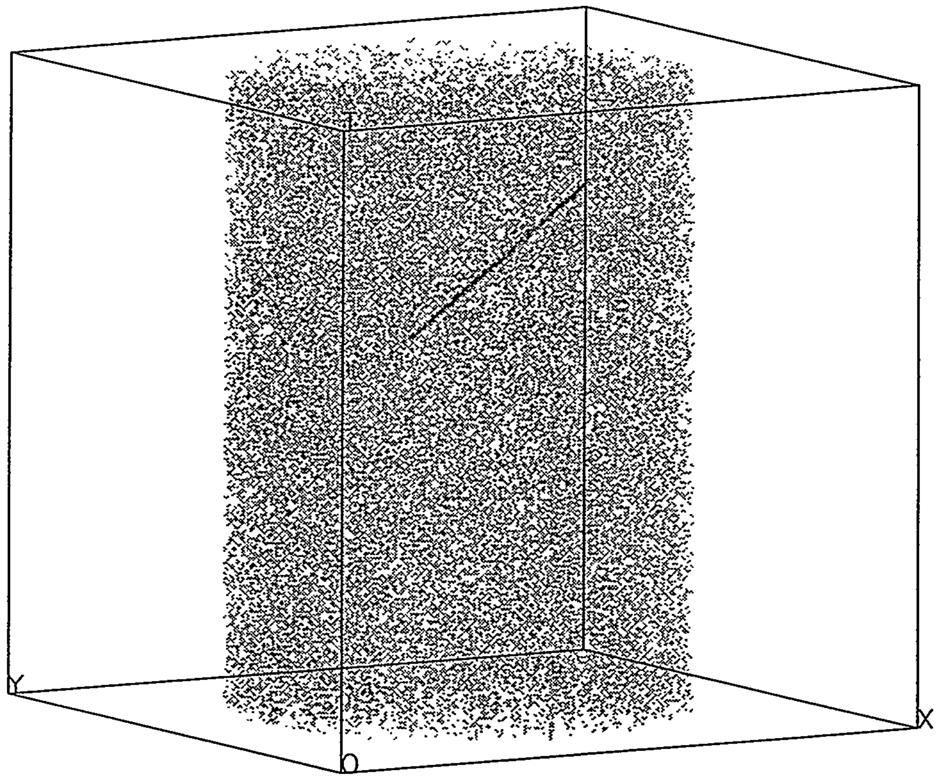

Fig. 5 – Three dimensional view of the data set of Figure 4.

6 shows the surface plot of a portion of the projected plane near the orbiting object. The zoomed region is 5 arcmin on the side. The total counts for this object during the 1 second transit time is about 1500 counts. In contrast, a neighboring region with the same area in the projected plane contains about 30 counts. The point source in the projected plane has a FWHM of about 1.2 arcmin, consistent with the measured FWHM from field stars. The significance of this object, based on an estimate image size of 1.5 by 1.5 arcmin, is much more than 500σ.

The orbiting object has an estimated count rate of about 1500 counts/sec. Scaling to HR6638 in Figure 3 yields a brightness of about 4th magnitude. It is moving at an estimated angular velocity of 46 arcminutes/sec. Assuming that the object is moving at a linear speed of 8 km/sec, the range is estimated to be 600 km. Assuming circular orbit, it is at an altitude of about 500 km. The direction of the motion indicates that this object has a very high inclination angle. This object was visible by naked eyes from a lighted site at Los Alamos National Laboratory (Jeff Bloch, private communication).

4. DISCUSSIONS

Comparison between figures 1 and 3 definitely demonstrates that additional dimensionality in the data set will help enhance the significance of linear features: We can clearly

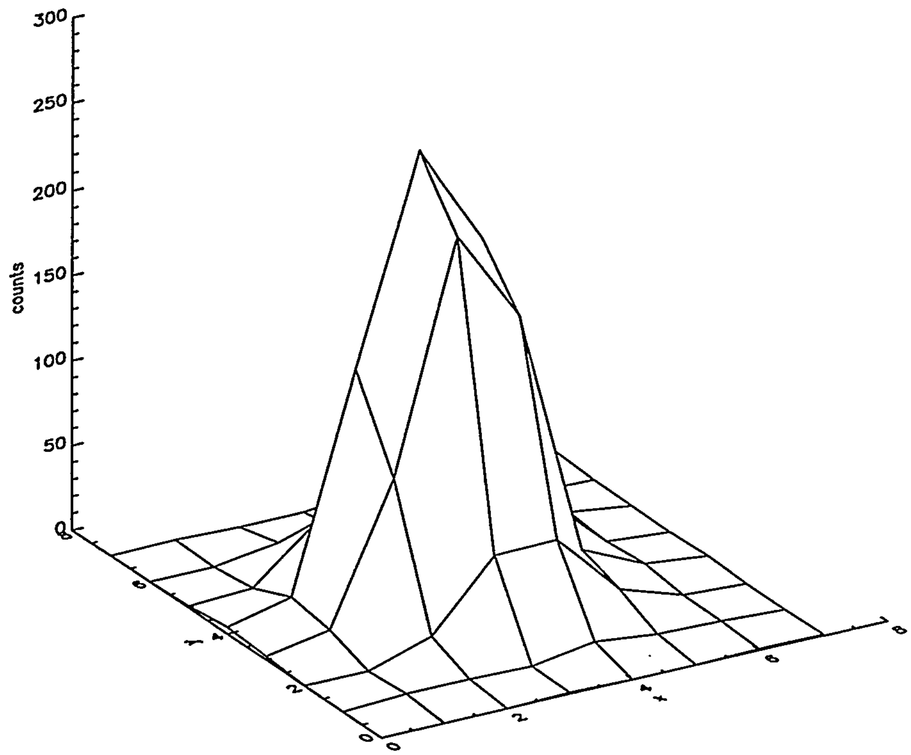

Fig. 6 – Surface plot of the area in the projected plane around the object.

see many more star-points in figure 3 than star-streaks in figure 1, keeping in mind that both figure are generated from exactly the same data set.

To further examine the sensitivity limit, let's examine figure 4. Some stars in Figure 4 have been identified. Specifically, the detected orbiting object passed through the star SAO 85583 of 7.7 magnitude near the bottom of the image. Other identified stars in this FOV are between 7th and 8th magnitude. This clearly indicates that we should be able to detect an orbiting object between 8th and 9th magnitude with this out-of-focus configuration.

We expect the sensitivity limit to improve from the following contributions.

1) The sensitivity limit scales linearly with the point source's FWHM. We foresee no difficulty in improving the FWHM by at least a factor of ten with a good tube and exposing in focus.

2) Figure 2 shows that we are not operating at the maximum count rate sustainable by the delay line readout and electronics (current system can support 5×10^5 counts/sec). The key reason is that the quantum efficiency has degraded significantly since the tube was built. (Skyward looking data collected during earlier field trips achieved a count rate in excess of 10^5 counts/sec.) A good tube with consistent QE will enhance the sensitivity limit, scaling roughly like the square root of the QE.

3) In the current analysis, the stellar photons are left in. Removing these photons will reduce the total number of background counts.

4) As mentioned earlier, the sky background is estimated to be 21 mag/square arcsec. With the July 5th observing site nestled between Los Alamos, Santa Fe and Albuquerque, city lights increase the sky background. The current detector system is mobile. And we plan to take the detector system to darker site for better observation condition in the future. We are also pursuing collaboration with existing debris monitoring site to mount our detector on existing telescopes.

Combining all of these factors, we do not anticipate difficulty in reaching the theoretical sensitivity limit projected between 15th to 16th magnitude.

In the field trips to date, we have acquired useful data to demonstrate the basic concept. More importantly, we have gained valuable experience which will help us perfect our observation procedure and develop an operational system. As with all developmental programs, experimental protocols continue to evolve. Mistakes such as not having the perfect focus and starting the exposure too late will no doubt be corrected as the project progresses.

As described in a previous paper (Ref. 1), data processing is a major challenge for this detection scheme. We have developed a prototype algorithm to handle the data analysis task and applied the algorithm to simulated data. However, the quality of data we have acquired to date is sub-optimal and we have chosen not to perform a full scale adaptation and optimization of the algorithm to these data sets. We expect to successfully fabricate another sealed MCP/CDL tube in the very near future. Field trips will soon follow and we fully anticipate the acquisition of high quality data. At that point we shall resume the algorithm development and adaptation to exploit the sensitivity of this space debris detection scheme.

ACKNOWLEDGEMENTS

We thank all team members of the MCP/CDL development and applications programs for their diligence in putting together a complex system. The Los Alamos debris detection project is supported by the US Air Force Phillips Laboratory's Debris Measurement Program. This work was performed under the auspices of US Department of Energy.

REFERENCES

1. Cheng Ho, William C. Priedhorsky, and Miles Baron, 1993, SPIE Proc. vol. 1951, p. 67.

2. Miles H. Baron and William C. Priedhorsky, 1994, SPIE Proc. vol. 2006, p. 188.

3. William C. Priedhorsky, et al. 1994, SPIE Proc. vol. 2006, p. 114.

DISCLAIMER